ISSN 2354-9114 (online), ISSN 0024-9521 (print)
Indonesian Journal of Geography Vol 55, No 3 (2023): 463-472
DOI: 10.22146/ijg.88213 website: https://jurnal.ugm.ac.id/ijg

INDONESIAN JOURNAL OF GEOGRAPHY

REVIEW ARTICLE

Source Determination of Debris Avalanche Deposit based on the Morphology and Distribution of Hummocky Hills on the Northeastern Flank of G. Sundoro and G. Sumbing, Central Java, Indonesia

Eti Rahayu[1], Haryo Edi Wibowo[1*], Mradipta Lintang Alifcanta Moktikanana[2], Agung Setianto[1], Agung Harijoko[1]
[1]Department of Geological Engineering, Universitas Gadjah Mada, Indonesia
[2]Department of Geosciences, Geotechnology, and Materials Engineering for Resources, Graduate School of International Resource Sciences, Akita University, Japan

Received: 2023-08-24
Revised: 2023-10-29
Accepted: 2023-12-04

Key words: hummocky hills, debris avalanche, morphometry, Sundoro, Sumbing

Correspondent email: haryo.edi.w@ugm.ac.id

Abstract The presence of hummocky hills as a typical product of debris avalanche deposits is prominently visible in the northeastern flank of G. Sundoro and G. Sumbing, Temanggung, Central Java. In an attempt to better understand the past behavior of both G. Sundoro and G. Sumbing, we identify the source of the debris avalanche deposit. Interpretation is performed on the basis of the assumption of two possible sector collapse sources, i.e., G. Sundoro and G. Sumbing. The Sumbing source scenario is assumed as freely spreading type considering 1) distribution of the hummocky hills are relatively on the northeastern flank of the volcano, and 2) the present crater structure on the summit of the volcano which is opening to the northeast. The Sundoro source scenario is assumed as valley-filling type considering the distribution of the hummocky hills are relatively on the eastern flank of Sundoro extended to the far distal area and bounded by older high topography of G. Sumbing and North Serayu Mountains. The source identification was done on the basis of field observation of the deposit lithological characteristics combined with image analysis, including hummocky hills morphometry, displacement angle, and spatial distribution. Image analysis identifies approximately 645 hummocky hills ranging from 1,851 m^z to 623,828 m^z and average of 23,482 m^2. Petrographic analysis of 5 representative block lava samples shows variation of olivine basalt, pyroxene andesite, to hornblende andesite. The results show that big size hummocky hills dominate the western side, while small size on the east. Displacement angle varied following the valley orientation with typical downslope topography. These suggested that the hummocky hills were originated from G. Sundoro as a valley-filling debris avalanche deposit.

1. Introduction

Besides volcanic eruptions, volcanic sector collapse is another potential for highly catastrophic volcanic disasters (Yoshida, 2014). Volcanic sector collapse is a large-scale and extremely rapid landslide that may cause thousands of cubic of rock mass to move up to tens to hundreds of kilometres cubic in minutes (van Wyk de Vries & Davies, 2015). The event of volcanic debris avalanche was recorded scientifically for the first time along with the 1980 eruption of Mt St Helens (Voight et al, 1981; Glicken, 1996), thus the study of this phenomenon was developing since then (Siebert, 1984; 2002; Yoshida et al, 2010; 2012; Yoshida, 2014; Paguican et al, 2014; van Wyk de Vries & Davies, 2015; Hayakawa et al, 2018; Paguican et al, 2020). The debris avalanche deposit may form a typical hummocky hills landform as the signature of past sector collapse event (Hayakawa et al., 2018).

The presence of hummocky hills topography is prominently visible in the northeastern flank of neighboring G. Sundoro and G. Sumbing. The hummocky hills are distributed in the vicinity of a highly populated area of Temanggung and Magelang Regency, Central Java. To this day, the origin of these hummocky hills is debatable. Van Bemmelen (1949) and Siebert (1984) stated that the hummocky hills were formed by a sector collapse event of G. Sundoro. However, that hypothesis was not further explained. Sukhyar et al (1992) defined the hummocky hills as a volcanic activity much older than G. Sumbing and G. Sundoro. Sitorus et al (1994) in the Geological Map of Sumbing Volcano mentioned that these hummocky hills deposits belong to Petarangan Debris Avalanche, while Prambada et al. (2016) believe that they are the product of G. Sumbing.

According to previous studies, there are some relationships between the morphometry and spatial distribution of debris avalanche deposits with the source of sector collapse (Yoshida et al, 2010; 2012; Yoshida, 2014; Hayakawa et al, 2018). Therefore, in this contribution, we aim to identify the source of the debris avalanche deposit on the basis of its deposit lithological characteristics combined with hummocky hills morphometry and spatial distribution analysis. Determination of the source of debris avalanche deposit on the northeast of G. Sundoro and G. Sumbing is important to better understand the past behavior of both volcanoes and the mechanism of sector collapse. These understanding are crucial to the future attempt of volcanic disaster risk prevention and mitigation.

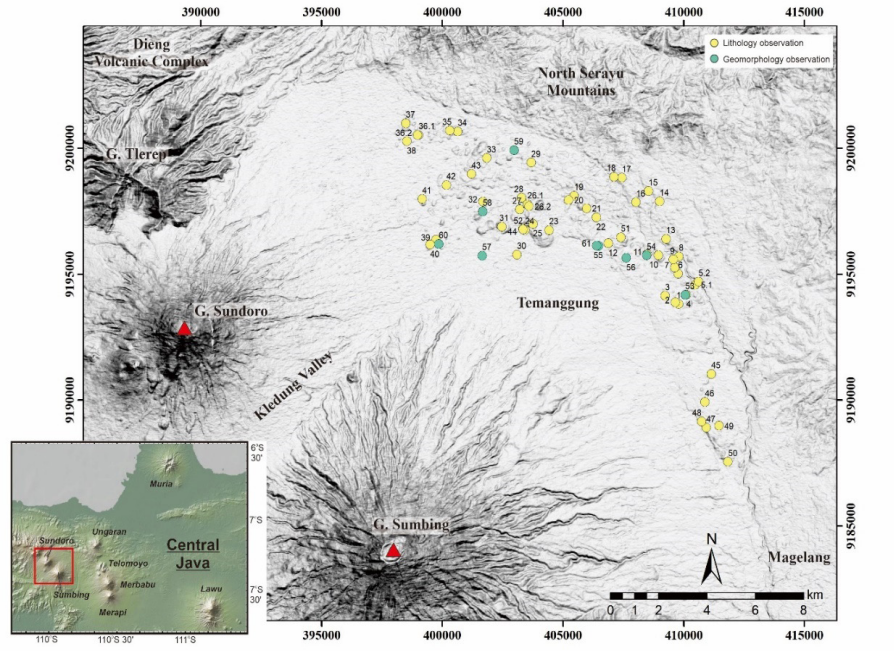

Figure 1. Location of the study area, northeast of G. Sundoro and G. Sumbing in Temanggung, Central Java, Indonesia. Coordinate in UTM Zone 49S.

2. Regional Geology

G. Sundoro (3136 masl) and G. Sumbing (3371 masl) are part of Java Quaternary volcanoes in the middle of the Central Depression Zone (van Bemmelen, 1949). These two volcanoes are part of the northwest-southwest volcanic alignment of, from oldest to youngest, Dieng Volcanic Complex, G. Sumbing, and G. Sundoro. Thus, naturally, the neighboring volcanoes of G. Sundoro and G. Sumbing are bordered by the Dieng Volcanic Complex to the west, North Serayu Mountains to the north, G. Merapi-G. Merbabu-G. Ungaran to the east and South Serayu Mountains to the south (Figure 1). The morphology of G. Sundoro shows an ideal stratocone with an overlapping eruptive crater on its summit. Some parasitic cones of G. Sundoro are distributed on the southwestern to western flanks, such as Kembang, Kekep, Watu, Arum, and Kebonan (Prambada et al., 2016). Meanwhile, G. Sumbing morphology consists of four volcanic edifices, from the oldest to youngest Old Sumbing, Beser Cone, Gianti Cone, and Young Sumbing (Sukhyar, 1989). G. Sumbing has a horse-shoe-shaped crater opened to the northwest, with a lava dome growing inside the crater toward the same direction.

The hummocky hills are distributed from the northeast to the southeast distal flank of G. Sundoro, or from the north to the east distal flank of G. Sumbing (Figure 2). Prambada et al. (2016) reported that those hummocky hills have dimensions of <500 m diameter and <100 m height, covered by >2 m thick soil, indicating a quite old sector collapse. Thanden et al. (1975) suggested the hummocky hills as part of the Old Sundoro Rock Formation (Qos) and consists of reworked, weathered pyroclastic rocks, suspected as lahar deposits. The Old Sundoro Rock Formation is surrounded by Sundoro Volcanic Rock (Qsu), which consists of hypersthene-augite andesite and olivine-augite basalt. Sukhyar et al (1992) describe the hummocky hills as part of an Old Volcanic Product (VTI) formed by fractured lava and surrounded by Alluvium. Sitorus et al (1994), suggested these hills are classified as Petarangan Debris Avalanche (Pda) and composed of massive lava blocks and columnar jointed lava.

3. Methods

Image analysis was conducted to identify and delineate the morphology of individual hummocky hills. We used multi-directional hillshade image processed from digital elevation map data (DEMNAS) from Indonesia Geospatial Portal, combined by Google Earth image and ESRI World Hillshade. Area, height, major axis, minor axis, elongation ratio, distance, direction, and displacement angle of the hummocky hills were examined according to the parameters in Yoshida et al (2010; 2012), Yoshida (2014), and Hayakawa et al (2018). In order to clearly identify the alignment and displacement angle of hummocky hills, the most representative hummocky hills morphometry data are chosen based on elongation ratio greater than 1.5. The measurement of distances from source are separated for both avalanche sources. The displacement angle was measure by the assumption of two different sector collapse source of G. Sundoro and G. Sumbing. The assumed source from G. Sundoro applied valley filling debris avalanche due to morphological barrier of G. Sumbing on the south and North Serayu Mountains on the north causing mechanism with 3 changing main flow direction (MFD); MFD 1 to the northeast (N60°E), MFD 2 to the east (N100°E), and MFD 3 to the southeast (N160°E) (Figure 2a). On the other hand, the assumption of Sumbing source applied the mechanism of freely spreading debris avalanche with individual flow direction (IFD) approximately to N40°E, align with both the opening of Sumbing Young Crater and inferred morphology of Sumbing Old Crater (Figure 2b). Image processing and GIS analysis were conducted using ArcMap 10.4, ArcGis Pro 2.0, and Global Mapper 19.

Fieldwork was performed in 61 observation points, including morphological, lithological and deposit structure observation (Figure 1). Rock samples were carefully observed under loupe (4x magnification) to identify the various mineralogical composition. The petrographic analysis was then conducted to five representative samples to confirm the lithological variation following igneous rock classification of

Clark (1966). The preparation and analysis were done in Get-In Cicero Laboratory, Geological Engineering Department, Universitas Gadjah Mada. Modal mineralogical variation was calculated with point counting method using J-Microvision 1.7 software for a total of 1000 points for each sample.

4. Result

Fieldwork

The hummocky hills in the northeastern side of Sundoro and Sumbing generally consist of block facies and mixed facies of debris avalanche deposit. Block facies is characterized by the presence of fractured lava blocks forming jigsaw crack and jigsaw fit structure with various intensity (Figure 3a and 3b), while mixed facies is a mixture of clastic angular blocks that break down during transportation, massive, unsorted, and contains clastic debris with a size of millimetres to meters (Figure 3c). The debris avalanche deposit is incised by fluvial activity in the form of lahars, varies from breccia, sandstone, and conglomerate (Figure 3d and 3e).

Mineralogy

The rocks composing the hummocky hills dominantly consist of lava blocks and volcanic breccia. Lava blocks range from olivine basalt, pyroxene andesite to hornblende andesite in composition. Porphytitic, trachytic, and hyalopilitic were commonly observed in the lava block samples. The mineral phases are plagioclase, orthopyroxene, clinopyroxene, olivine, hornblende, and Fe-Ti oxide. Summary of modal mineralogical composition are presented in Table 1. Oscillatory zoning, patchy zoning, and sieve are present in plagioclase. Opacitic rim is present mostly in pyroxene, but fewer in hornblende. Groundmass is mainly composed of volcanic glass and plagioclase microlite. Photomicrograph of the representative samples are presented in Figure 4.

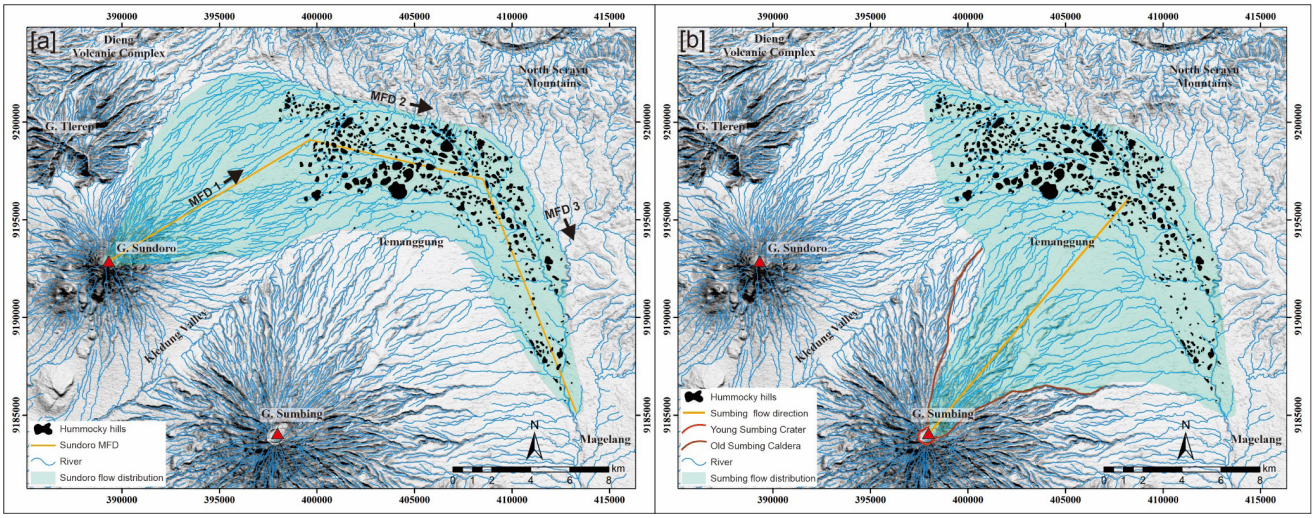

Figure 2. The distribution of debris avalanche deposits and hummocky hills surrounding G. Sundoro and G. Sumbing. The flow was bordered by Dieng Volcanic Complex and North Serayu Mountains in the north. [a] Assumption of G. Sundoro source applies changing to three main flow directions: MFD 1 to the northeast, MFD to the east, and MFD 3 to the southeast. [b] Assumption of G. Sumbing source applies main flow direction to the northeast with individual flow direction for each hummocky hills.

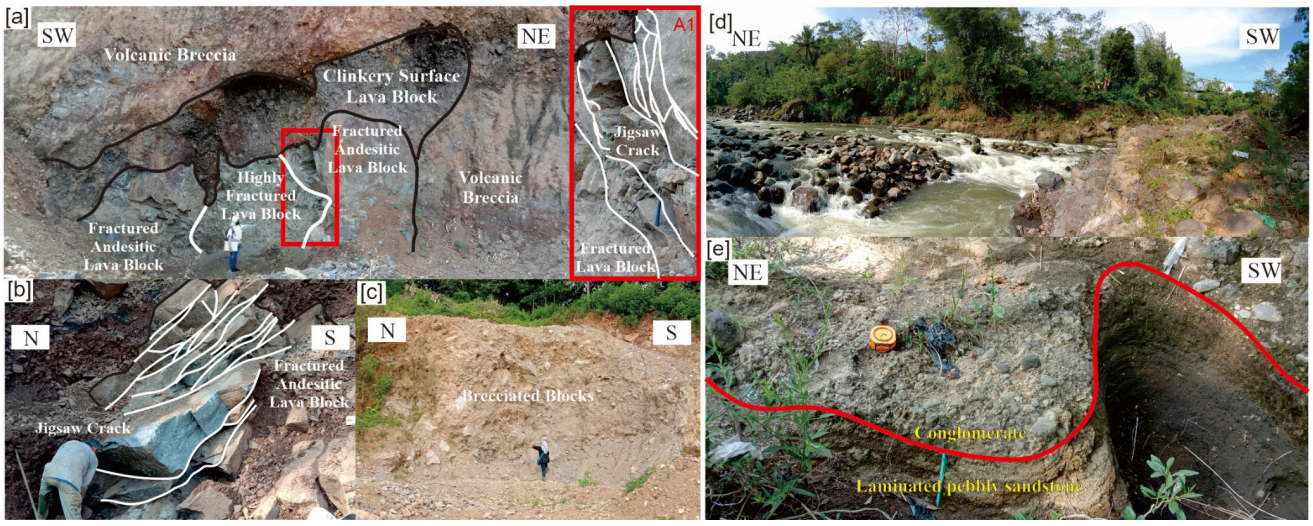

Figure 3. Various appearance of jigsaw cracks in G. Sundoro – G. Sumbing hummocky hills. [a] Irregular jigsaw cracks on andesitic lava. fracture density varies from moderate to very intense. [b] Regular jigsaw cracks. (c) The outcrop of mixed facies, consists of brecciated blocks as fragment and fine-grained volcanic material as matrix. (d) River incision in the middle of the debris avalanche deposit. The river deposited lahar in the form of laminated pebbly sandstone and conglomerate.

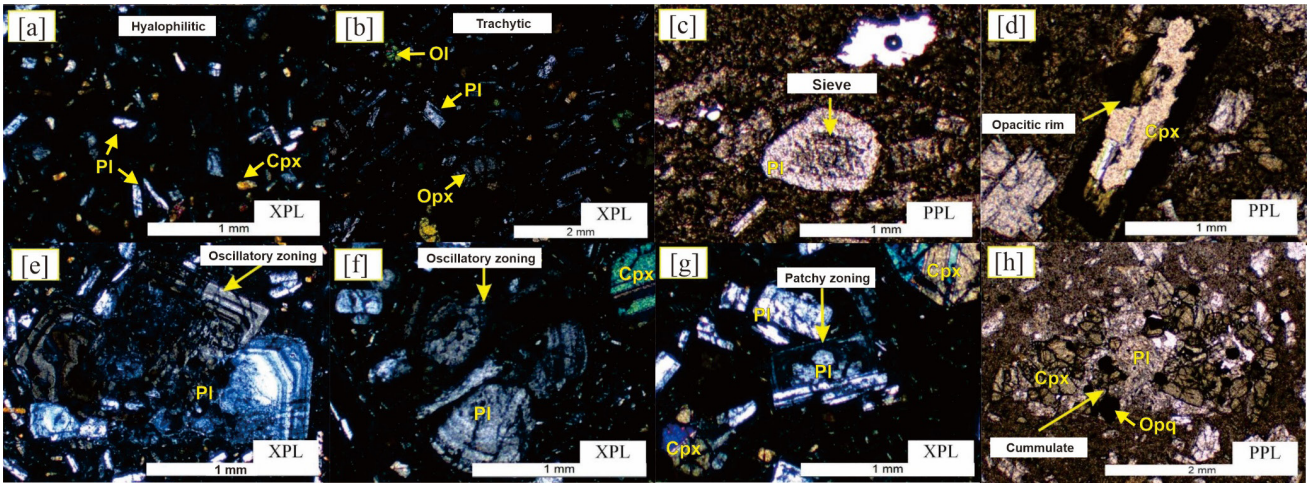

Figure 4. Photomicrograph of rock and mineral textures in lava block samples. [A] Hyalopilitic texture in andesite. [B] Trachytic texture in basalt. [C] Sieve texture in plagioclase. [D] Opacitic rim in clinopyroxene. [E-F] Oscillatory zoning in plagioclase [G] Patchy zoning in plagioclase [H] Cummulate texture of plagioclase, clinopyroxene, and opaque minerals.

Table 1. Modal mineralogical composition (in vol%) and mineral textures based on petrographic observation. Pl: Plagioclase, Cpx: Clinopyroxene, Opx: Orthopyroxene, Hb: Hornblende, Ol: Olivine, Opq: Opaque minerals, Fe-ox: Fe-oxide, GM: Ground Mass, Vsc: Vesicle.

Sample	H 44 (Ol Basalt)	H 45 (Px Andesite)	H 47 (Hb Andesite)	H 48 (Ol Basalt)	580 (Hb Andesite)
Pl	26	29	21	23	29
Cpx	8	11	1	3	5
Opx	9	12	5	1	11
Hb	-	-	6	<1	11
Ol	10	-	-	8	-
Opq	6	9	4	4	8
Fe-ox	-	8	<1	21	6
GM	34	24	39	23	34
Vsc	7	9	24	16	6
Texture	trachytic	hyalophilitic	hyalophilitic	trachytic	hyalophilitic

Hummocky hills morphometry

Morphometry analysis was conducted on a total of 645 hummocky hills with area ranges from 1,851 m^2 to 623,828 m^2 and average of 23,482 m^2. The hummocky hills' major and minor axis ranges from 59 to 961 m and 40 to 875 m, respectively, and its height varies from 10 to 113 m. While hummocky hills distance (from the assumed source) ranges from 10,684 to 24,604 m and 11,371 to 18,620 m for Sundoro and Sumbing, respectively (Figure 5). Using a cumulative probability plot, the size of the hummocky hills is then categorized into 3 classes: small, medium, and big. The small hummocky hills have an area of less than 5000 m^2, medium size ranges from 5000 to 63,000 m^2, and the big ones are those that are larger than 63,000 m^2. The data of hummocky hills' size and displacement angle is then interpolated by Natural Neighbour to generate some distribution maps representing changes in size and displacement angle on the basis of spatial distribution, as well as its connection with slope and surrounding morphology. Five topographic profiles were constructed from the collapse source, passing through the MFDs and perpendicular to the hummocky hills distribution area to give a general picture of the slope condition, morphology, and how they affect the sector collapse mechanism.

Distance from source

The correlation between hummock size and distance from each source was plotted in bivariate diagrams (Figure 5). Assuming Sundoro as the source (Hereafter referred to as Sundoro scenario), we observed the following features: (1) the small hummocks are more numerous at larger distance; (2) medium hummocky hills are not showing any particular pattern, with relatively uniform distribution both at close and long distances; and (3) the big hummocky hills showing a pattern of enlargement to the center of MFD2 and then decreasing from MFD2 to MFD3. Under the assumption that the hummocks originate from Sumbing (Hereafter referred to as Sumbing scenario), we found that the small and medium hummocky hills show uniform distribution both at close and long distance, while the big hummocky hills' size decreases along with the increasing distance from the source.

The relationship between hummocky hills size and distance from the source is also presented in the distribution map (Figure 6a and 6b). For Sundoro scenario, we observed distinct patterns of hummocky hill size in each MFD area. In the MFD1, bigger hummocky hills are situated at a closer. Hummocky hills size progressively increased towards the central part of MFD2 area, and smaller hummocky hills are

scattered on the marginal side of MFD2 area, bordered by North Serayu Mountains. In the MFD3 area, the hummocky hills size is larger and smaller at the beginning and end of the flow, respectively (Figure 6a). While the Sumbing scenario shows that larger hummocky hills are dominantly present in the west and smaller hummocky hills are distributed mainly in the east (Figure 6b).

Slope

The mechanism of avalanche flow represented by spatial distribution and displacement angle of hummocky hills is affected by the slope condition along the flow (Yoshida, 2014). Therefore, 5 topographical sections were constructed to present slope conditions along the debris avalanche flow and its influence on the flow regime (Figure 7 and Figure 8).

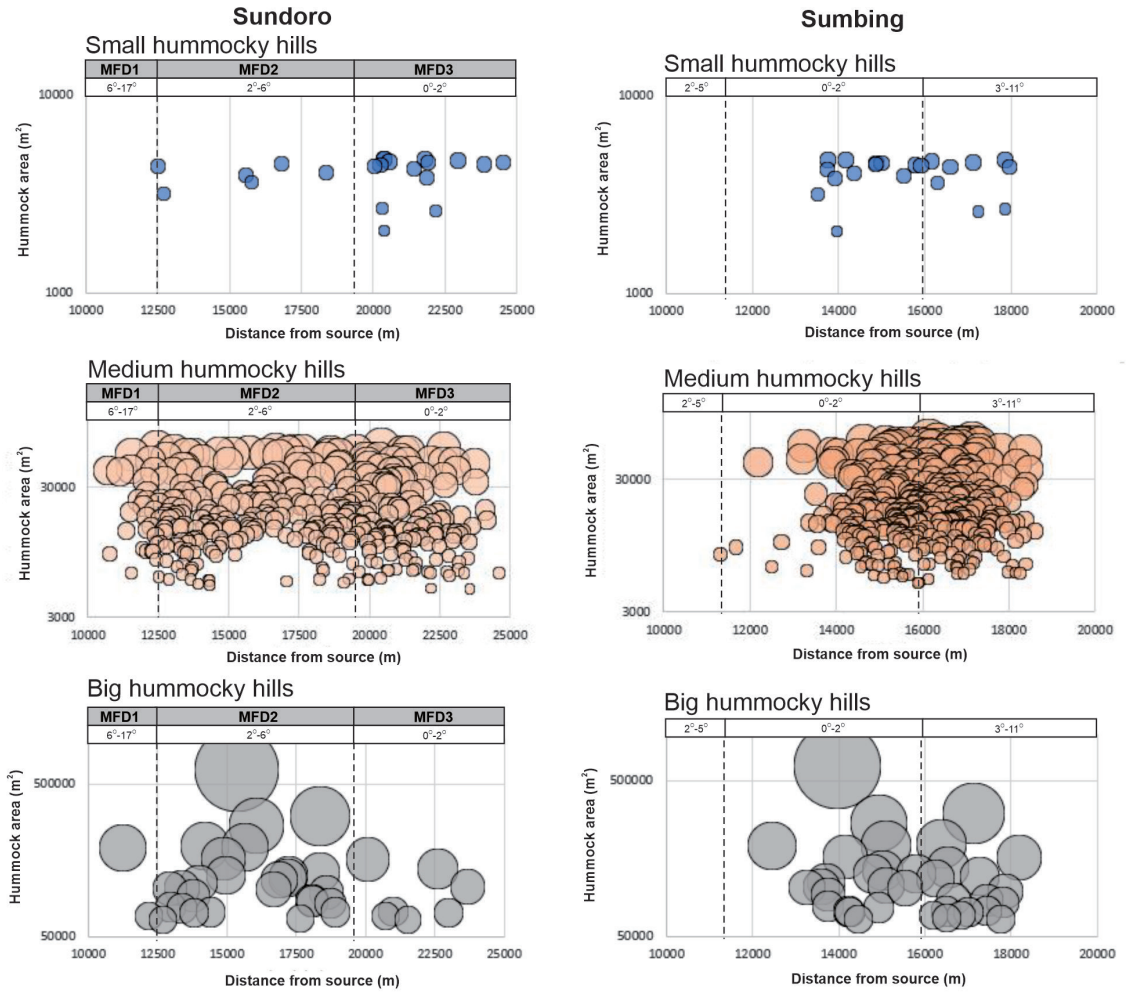

Figure 5. Bivariate diagram of hummocky hills' size and distance from G. Sundoro and G. Sumbing, with distinct patterns for both sources. From G. Sundoro, small hummocks are more abundant at longer distance. Medium hummocky hills are uniformly distributed along the distance. Big hummocky hills show enlargement in MFD2 and downsizing in MFD3. From G. Sumbing, small and medium hummocky hills show uniform distribution, while big hummocky hills get smaller at further distances.

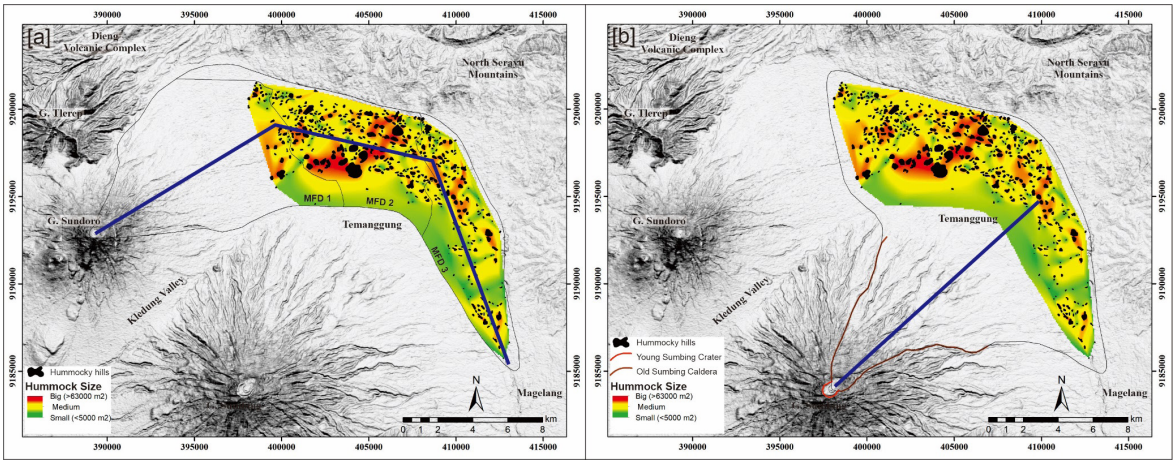

Figure 6. [a] Size distribution map of hummocky hills assuming source from G. Sundoro. The size of hummocky hills become larger in MFD2. Smaller hummocky hills are scattered on the side of MFD2. In MFD3, hummocky hills size is larger in the beginning of flow and become smaller at the end. [b] Size distribution map of hummocky hills assuming source from G. Sumbing. Big hummocky hills are mainly distributed in the west, while small hummocky hills dominate the eastern part.

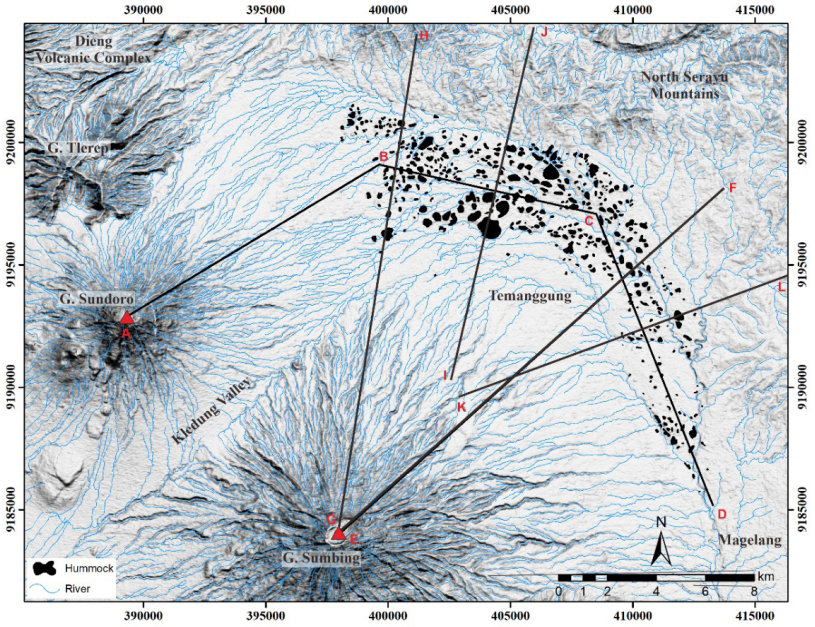

Figure 7. Location of the extracted topographic profile around G. Sundoro and G. Sumbing

Section ABCD was made parallel to the debris flow's direction, under the assumption of the Sundoro scenario (Fig. 7 and 8) Here, the slope became gentler along with more distance from the avalanche source. MFD1, which is closer to the avalanche source, has a slightly steep to steep slope (>6-30°). In MFD2, the slope changes to gentle (>2-6°) and becomes flat (0-2°) in MFD3. Hummocky hills are located within the area of a slightly steep to flat slope. Section EF is also parallel to the debris flow's direction, but under the assumption of Sumbing as the potential source (Fig. 7 and 8). The results are similar to the Sundoro scenario, where a steeper slope (>5-35°) is typically observed at a closer distance to the avalanche source and genter slope (0-2°) is observed in the hummocky hills area. Going further, the slope becomes steeper again, in which observed in the North Serayu Mountains.

Section GH-IJ-KL were created perpendicular to the flow of Sundoro. It is shown that the slope condition is slightly steep to steep (~5-35o) in the southwestern and northeastern parts due to the presence of G. Sumbing and North Serayu Mountains, respectively. Hummocky hills are emplaced in the gentle to flat valley between the two high topography.

Displacement Angle

Bivariate diagrams of the hummock displacement angle and distance from each assumed source are presented in Figure 9. The diagrams show that the data is randomly distributed, and the pattern of displacement angle is not clearly visible. Therefore, a distribution map of the displacement angle was made to present the spatial distribution in a map view in an attempt to identify which area has a dominantly parallel or perpendicular displacement angle in relation to the distance from source, slope condition, and pre-existing morphology. The distribution map of Sundoro assuming source shows that displacement angle has a distinct pattern on each MFD (Figure 10a). MFD1 at the beginning of avalanche flow is dominated by a perpendicular displacement angle. The outside of the bend of MFD2, bounded by the North Serayu Mountains, shows a parallel displacement angle, while the inside of the bend of MFD2, bounded by G. Sumbing, is more perpendicular. The central part of MFD3, confined by the high topography of G. Sumbing and North Serayu Mountains, is dominated by parallel displacement angle, while at the end of MFD3, the displacement angles are more perpendicular. On the other hand, the displacement angle distribution map from the Sumbing scenario shows that perpendicular displacemen t angles and parallel ones are clustered in the western and eastern parts, respectively (Figure 10b).

5. Discussion

Hummocky hills lithological characteristics

Volcaniclastic deposit that forms the hummocky hills is showing the characteristics of a debris avalanche deposit as indicated by the jigsaw cracks and jigsaw fit structure in the block facies. The studied hummocky hills consist of both block and mixed facies. Block facies are varied from olivine basalt, pyroxene andesite, and hornblende andesite. These lithological variations are within the range of those of Sundoro, either lava or pyroclastic flow breccia, as reported by Sukhyar et al. (1992), Prambada et al. (2016), and Wibowo et al. (2022), Sitorus et al. (1994) reported that Sumbing rocks are mostly andesite pyroxene to andesite hornblende. Minor basalt are reported as fragment in the pyroclastic flow breccia with no information of olivine content. Dempsey (2012) reported the rock of Sumbing range from basaltic andesite to andesite and no reported occurrence of olivine. Mixed facies are mainly composed of clastic angular blocks that break down during transportation, and clastic debris with a size of millimeters. These compositional variations and the unique structure are typical debris avalanche deposits of stratovolcano (Ui, 1983; Siebert, 1984; 2002; van Wyk de Vries & Davies, 2015).

Source of the debris avalanche deposit

Assuming the debris avalanche flow originated from G. Sumbing, we may consider that the flow mechanism is freely spreading debris avalanche. Based on the freely spreading model, a bigger hummock size should dominate in the central part of the flow, and align with the direction of sector collapse crater opening (Yoshida, 2014). Figure 8 shows that big size hummocky hills started to appear in the 12 km distance and shows a decreasing trend from 14 to 18 km distance. However,

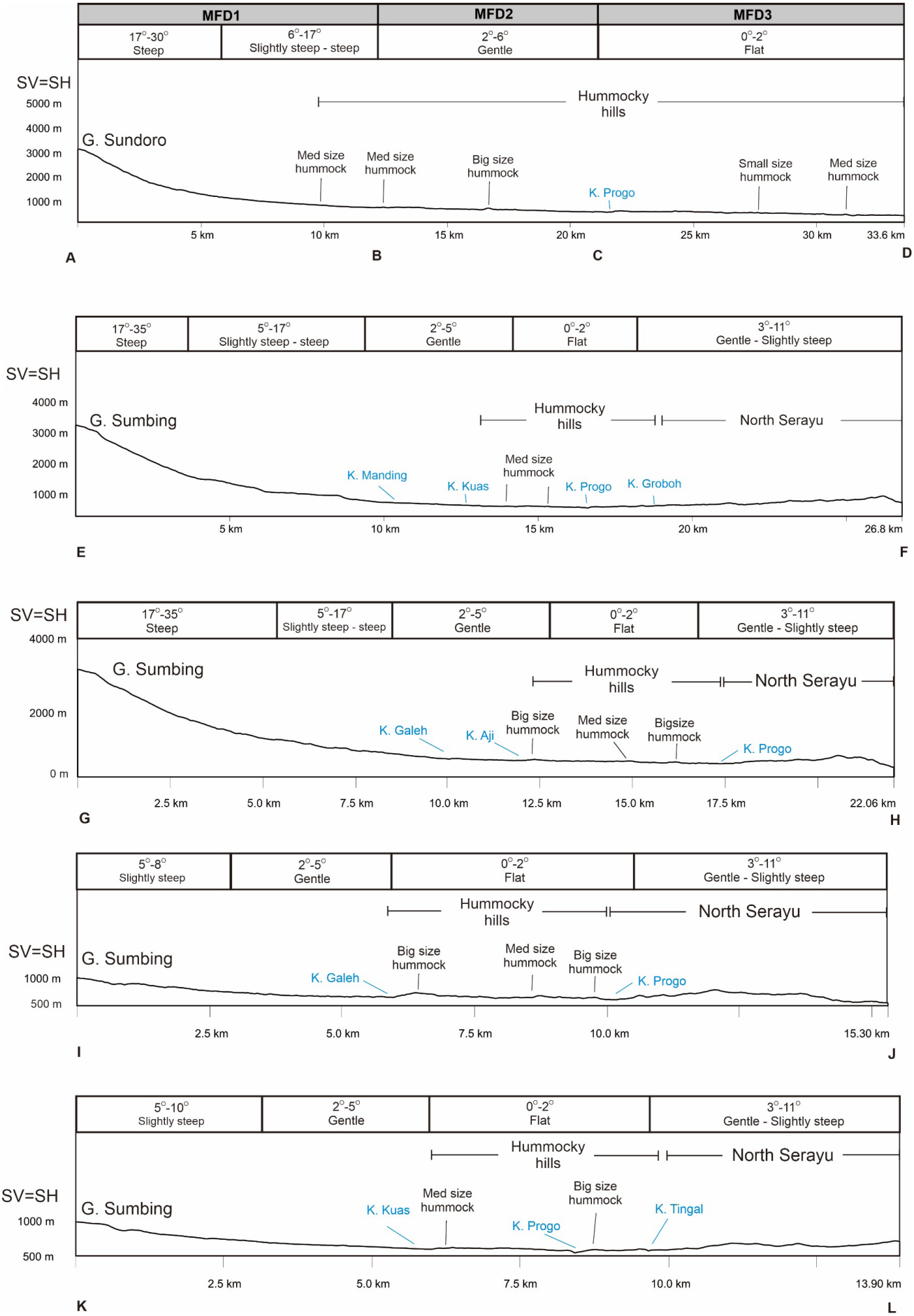

Figure 8. Topographic profile of G. Sundoro and G. Sumbing. ABCD represents G. Sundoro flow direction. EF represents G. Sumbing flow direction. GH, IJ, and KL are perpendicular to G. Sundoro flow direction and hummocky hills distribution. Hummocky hills are distributed on the gentle to flat slope, bordered by slightly steep to steep slopes of G. Sundoro, G. Sumbing, and North Serayu Mountains.

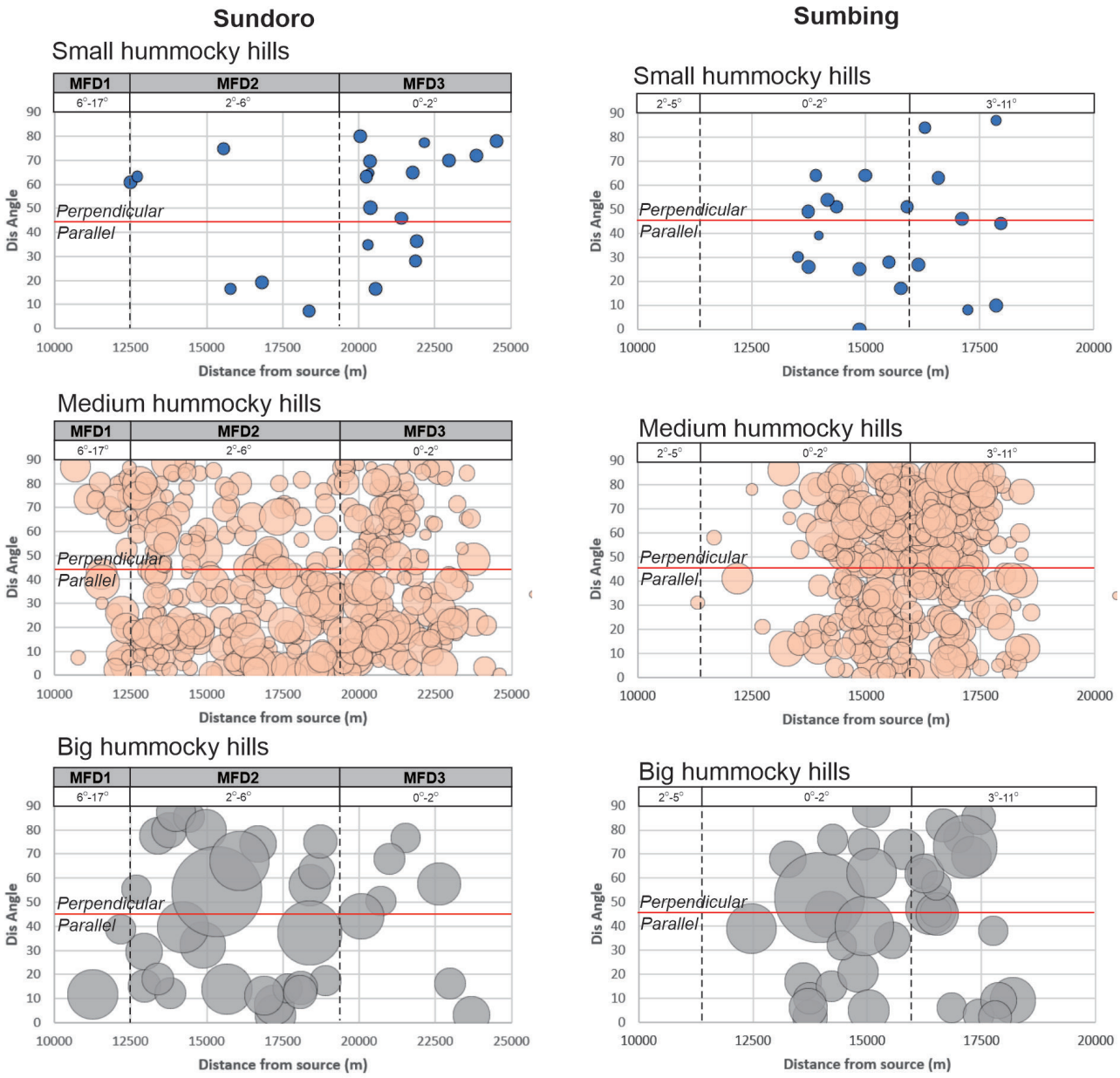

Figure 9. Bivariate diagram of hummocky hills' displacement angle and distance from G. Sundoro and G. Sumbing. The bivariate plots do not shows any trends between distance from the source and displacement angle.

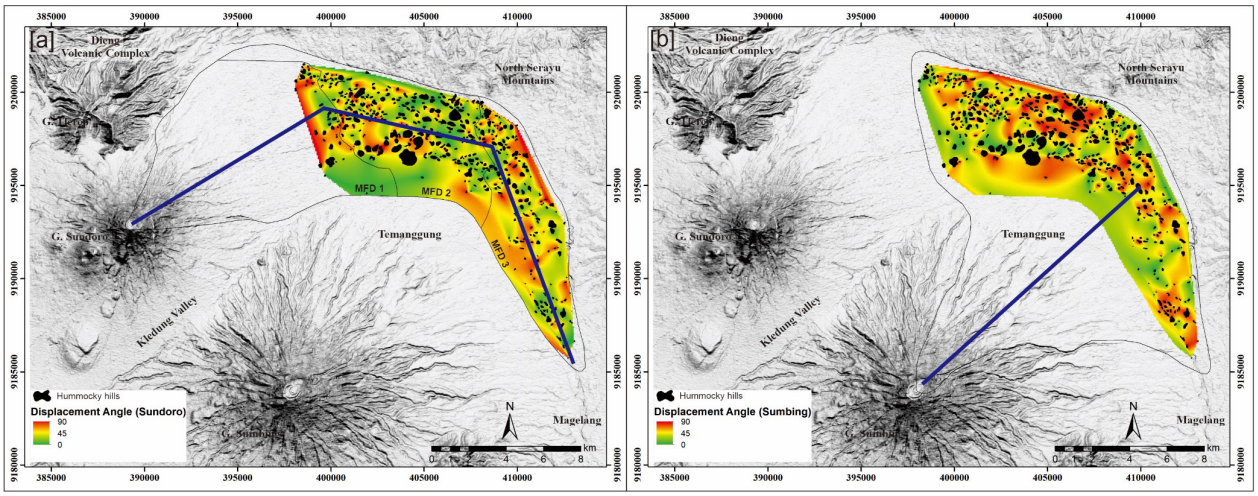

Figure 10. [a] Hummocky hills displacement angle map assuming the source from G. Sundoro. Perpendicular displacement angle is distributed at the beginning of avalanche flow on MFD1 to early MFD2, southern part of MFD2, and the edges of MFD3. Meanwhile, parallel displacement angle is distributed in the northern part MFD2 and central part of MFD3. [b] Hummocky hills displacement angle map assuming the source from G. Sumbing. Perpendicular displacement angle is dominating the western part while parallel displacement angle is mainly in the eastern part.

the distribution map shows that the larger size hummocky hills are distributed mainly on the western side while the medium to small sizes are in the eastern side. The distribution of big-size hummocky hills is mostly to the west of the flow direction (Figure 6b). This uneven size distribution does not match with the freely spreading debris avalanche model. In addition, a freely spreading mechanism will produce both parallel and perpendicular displacement angles which are distributed evenly throughout the area (Yoshida, 2014; Alfin et al., 2022). Figure 10b shows that the displacement angle is not distributed evenly where the perpendicular angle is mainly distributed to the west while the parallel angle is dominantly on the eastern part of the flow.

Assuming the debris avalanche flow originated from G. Sundoro, we may consider that the flow mechanism is valley-filling debris avalanche, where the hummocky hills are bounded by the older topography of North Serayu Mountains in the north and G. Sumbing in the south. This condition is well depicted by the distribution of hummocky hill size at each MFD zone (Figure 6a). MFD 1 zone shows a typical pattern of debris avalanche flow, with larger hummocky hills emplaced at the beginning of the flow within a closer distance. The avalanche flow continues to the MFD 2 zone where the size of the hummocky hill become larger within the central or inside of the bend of the flow due to the confined morphology of G. Sumbing and G. Sundoro that cause a shift of main flow direction from MFD 1 (SW-NE) to MFD 2 (NW-SE) and then to MFD 3 (NNW-SSE). Change of flow direction may reduce the flow velocity in the inside convex so that fragmentation will be very minimum. It is likely that the flow velocity on the outer convex part is relatively faster, allowing an extensive fragmentation and yields a dominantly small size of hummocky hills. Hummocky hills size are big at the beginning of MFD 3 flow and gradually decrease along the flow. At the end of the MFD 3 zone, the morphological barrier is absent, thus maximum energy release and intensive fragmentation may occur. The valley-filling mechanism may produce various displacement angles following the change of the directional flow and slope condition. Following the model of hummock orientation to slope condition of Yoshida (2014), we may expect that the displacement angle on the MFD 1 zone are mostly perpendicular due to decreasing slope. On MFD 2 and 3 zone, the slope is decreasing to constant so the displacement angle should be parallel. Figure 10a shows that the pattern on MFD 1 fit with expected model with a perpendicular displacement angle at the beginning of the flow. The displacement angle on the outside of the bend of MFD 2 became parallel because the hummocky hills were aligned with the main flow direction that is bordered by North Serayu Mountains, and the slope is decreasing to constant. While the displacement angle on the inside of bend of MFD 2 is primarily perpendicular. This might affected by the initial topography of G. Sumbing whose slope is relatively perpendicular to the flowing direction. On the middle part of MFD 3, the displacement angle is relatively parallel because of the constant slope, so that the alignment of the hummocky hills would follow the main flow direction. On the edge of the MFD 3 zone, the hummocky hills displacement angle is relatively perpendicular as typical of the outer edge of debris avalanche deposit. In general, the distribution and orientation of the hummocky hills match the model expected from valley filling debris avalanche mechanism coming from G. Sundoro.

Debris avalanche related to flank or sector collapse is part of cyclic growth of a volcano with recurrence rate range from hundreds to thousands years and even thousand to tens thousands years (Zernack and Procter, 2021). Post collapse regrowth of a volcano might partly to fully covered up the amphitheatre morphology of a collapse event i.e. Mt. Fuji, Mt. Komagatake, and Mt. Akagi, Japan (Yoshida et al., 2014). Thus, the absence of identifiable amphitheatre structure on the summit and the eastern flank of G. Sundoro might indicates the intense regrowth process after the collapse event.

6. Conclusion

The hummocky hills on the northeast of G. Sundoro and G. Sumbing are characterized as debris avalanche deposits from volcanic sector collapse phenomena. This deposit consists of block facies and mixed facies. Block facies are mainly composed of basaltic to andesitic lava blocks and volcanic breccia with jigsaw crack structures. The distribution of size and displacement angle of the hummocky hills on the northeast of G. Sundoro – G. Sumbing is matched with the scenario using G. Sundoro source assumption with valley filling debris avalanche mechanism. The absence of amphitheatre or collapse scar on the eastern flank of G. Sundoro may be related to the high growth rate of the volcano after the collapse event.

Acknowledgement

This study is fully funded by Geological Engineering Department Gadjah Mada University Research Grant, year 2020. We also would like to thank Muhammad Farid Darmawan, Dina, and Rifqi Prasanda Whido Saputro for their assistance during fieldwork.

References

Alfin, A. S., Wibowo, H. E., Harijoko, A. (2022). Morphometric Characteristic and Distribution of Hummocky Hills in Debris Avalanche Deposit of Galunggung Volcano, West Java, Indonesia. *IOP Conference Series: Earth and Environmental Science* 1071, 012012

Clark, S.P., Jr., 1966. Composition of rocks. In: Clark, S.P., Jr., (Ed.), Handbook of Physical Constants. Geological Society of America Memoir 97, 1–5.

Dempsey, S. R. (2013). Geochemistry of volcanic rocks from the Sunda Arc. Durham theses. Durham University,

Glicken, H. (1996). Rockslide-debris avalanche of May 18, 1980, Mount St. Helens Volcano, Washington. *US Geological Survey Open-File Report 96–0677*, 1–90.

Hayakawa, Y. S., Yoshida, H., Obanawa, H., Naruhashi, R., Okumura, K., Zaiki, M., & Kontani, R. (2018). Characteristics of debris avalanche deposits inferred from source volume estimate and hummock morphology around Mt. Erciyes, Central Turkey. Natural Hazards and Earth System Sciences 18, 429–444. https://doi.org/10.5194/nhess-18-429-2018

Paguican, E. M. R., van Wyk de Vries, B., & Lagmay, A. M. F. (2014). Hummocks: How they form and how they evolve in rockslide-debris avalanches. *Landslides* 11(1), 67–80. https://doi.org/10.1007/s10346-012-0368-y

Paguican, E.M.R., Roverato, M., Yoshida, H. (2021). Volcanic Debris Avalanche Transport and Emplacement Mechanisms. In: Roverato, M., Dufresne, A., Procter, J. (eds) *Volcanic Debris Avalanches.* Advances in Volcanology. Springer, Cham. https://doi.org/10.1007/978-3-030-57411-6_7

Prambada, O., Arakawa, Y., Ikehata, K., Furukawa, R., Takada, A., Wibowo, H. E., Nakagawa, M. & Kartadinata, M. N. (2016). Eruptive history of Sundoro volcano, Central Java, Indonesia

since 34 ka. *Bulletin of Volcanology* 78, 81. https://doi.org/10.1007/s00445-016-1079-3

Siebert, L. (1984). Large Volcanic Debris Avalanches: Characteristics of Source Areas, Deposits, and Associated Eruptions. *Journal of Volcanology and Geothermal Research* 22 (3–4), 163–197. https://doi.org/10.1016/0377-0273(84)90002-7

Siebert, L. (2002). Landslides resulting from structural failure of volcanoes. In S G Evans, J V De Graff (eds) *Catastrophic landslides: effects, occurrence, and mechanisms*. Geological Society of America Reviews in Engineering Geology 15, 209–235.

Sitorus, K., Erfan, R.D., Bacharudin, R., & Mulyana, A. R. (1994). Geological Map of Sumbing Volcano, Central Java. Bandung: Volcanological Survey of Indonesia.

Sukhyar, (1989), Geochemistry and petrogenesis of arc rocks from Dieng, Sundoro, and Sumbing volcanic complexes Central Java, Indonesia. PhD thesis. Monash University, Australia.

Sukhyar, R., Sumartadipura, N.S., & Erfan, R.D. (1992). Geological Map of Sundoro Volcano, Central Java. Bandung: Volcanological Survey of Indonesia.

Thanden, R.E., Sumadirja, H., & Richards., P.W., 1975. Geologic Map of the Magelang and Semarang Quadrangle, Java. Bandung: Geological Survey of Indonesia.

Ui, T., (1983). Volcanic Dry Avalanche Deposits - Identification and Comparison with Nonvolcanic Debris Stream Deposits. *Journal of Volcanology and Geothermal Resources* 18 (1-4), 135-150. https://doi.org/10.1016/0377-0273(83)90006-9

van Bemmelen, R. W. (1949). *General Geology of Indonesia and Adjacent Archipelagoes*. The Hague: Government Printing Office.

van Wyk de Vries, B. & Davies, T. (2015). Landslides, debris avalanches, and volcanic gravitational deformation. In H Sigurdsson, B F Houghton, S R McNutt, H Rymer, & J Stix (eds) *Encyclopedia of Volcanoes* (p. 665–668). San Diego: Academic Press.

Voight, B., Janda, R. J., Glicken, H., & Douglas, P. M. (1981). Catastrophic Rockslide Avalanche of May 18, in P. W. Lipman & D. R. Mullineaux (eds) *The 1980 Eruption of Mount St. Helens, Washington* (p. 347-377). Washington DC: USGS Professional Papers.

Yoshida, H., Sugai, T., Ohmori, H. (2010). Longitudinal downsizing of hummocks by the freely spreading volcanic debris avalanches in Japan. *The Quaternary Research (Daiyonki-Kenkyu)* 49 (2), 55–67. https://doi.org/10.4116/jaqua.49.55

Yoshida, H., Sugai, T., Ohmori, H. (2012). Size–distance relationships for hummocks on volcanic rockslide-debris avalanche deposits in Japan. *Geomorphology* 136 (1), 76–87. https://doi.org/10.1016/j.geomorph.2011.04.044

Yoshida, H. (2014). Hummock Alignment in Japanese Volcanic Debris Avalanches Controlled by Pre-avalanche Slope of Depositional Area. *Geomorphology* 223, 67–80. https://doi.org/10.1016/j.geomorph.2014.06.024

Zernack, A. V. and Procter, J. N. (2020). Cyclic Growth and Destruction of Volcanoes. In Volcanic Debris Avalanches, Advances in Volcanology, Roverato et al., (eds.). 311-355. Springer Nature Switzerland. https://doi.org/10.1007/978-3-030-57411-6_12.